

Character of ground state of an aperiodic frustrated Josephson junction array

Y. Azizi,¹ M. R. Kolahchi,¹ and J. P. Straley²

¹ *Institute for Advanced Studies in Basic Sciences, Zanjan 45195-1159, Iran and*

² *Department of Physics and Astronomy, University of Kentucky, Lexington, KY, 40506, U.S.A.*

We study the energy spectrum for an aperiodic Josephson junction ladder, as a function of frustration. Frustration is brought about by application of a transverse magnetic field, and aperiodicity is imposed by the arrangement of plaquettes with two incommensurate areas. We study the effect of the incommensurate plaquette areas in conjunction with that of the aperiodicity. The structure of the energy spectrum at deep minima is shown to be described by a model that treats the plaquettes independently. The energy spectrum is a quasiperiodic function of frustration; short range correlations in the arrangement of plaquettes have a small effect on the energy power spectrum.

PACS numbers: 74.81.Fa, 61.44.-n, 61.43.-j, 61.43.Hv, 74.25.Qt

I. INTRODUCTION

The electronic and transport properties of quasiperiodic systems are affected by their quasicrystalline structure. In one-dimensional (1D) systems with Fibonacci order, the energy spectrum is singularly continuous and the wave functions are neither localized nor extended.¹ Similar exotic electronic states are predicted for the 3D icosahedral quasicrystals.² The structurally ordered icosahedral phases and their crystalline periodic approximants show the same transport properties, implying that the local configurational order (common in both) plays the major role.³ At the same time, study of the Fibonacci semiconductor superlattices indicates that at low enough temperatures, the longitudinal magnetoresistance of the quasiperiodic structure can be distinguished from that of its low order periodic approximant.⁴

In two dimensions, two types of study have been illuminating. One has been the study of the electronic structure, the energy spectrum and wave functions, which again has shown results similar as above, particularly in case of the two-dimensional (2D) Penrose lattice.⁵ The other kind is inspired by the Little-Parks effect,⁶ revealing the interplay of flux quantization and free energy and manifest in the variation of critical temperature of the 2D lattice as a function of the applied magnetic field perpendicular to its plane.^{7,8} Here, we consider the ground state of an aperiodic array of Josephson junctions, mainly drawing from the second type of study.

Josephson arrays give a useful context in which to study frustration. These are composed of weakly coupled superconductors, with an interaction between neighboring sites,

$$H = -E_J \sum_{\langle i,j \rangle} \cos(\theta_i - \theta_j - A_{ij}), \quad (1.1)$$

where θ is the phase of the superconducting order parameter on the site. A_{ij} describes the effect of the magnetic field; it is proportional to the line integral of the component of the vector potential along the link from i to j . It causes the phase of the superconducting wavefunction to vary from place to place. If we define the gauge invariant

phase differences $\Delta_{ij} = \theta_i - \theta_j - A_{ij} + 2n\pi$, where the integer n is chosen so that $-\pi < \Delta_{ij} < \pi$, it is readily seen that the Δ_{ij} cannot all be zero, because the directed sum of the A_{ij} around a plaquette is the magnetic flux through it. Further, it is found that the directed sum of the Δ_{ij} around a plaquette sometimes differs from the magnetic flux by a multiple of 2π ; we will say that these plaquettes contain a vortex. The ground state is specified by a configuration of vortices.⁹ Thus these systems exhibit frustration¹⁰, meaning that in the ground state, the individual terms of Eq. (1.1) are not simultaneously at minimum.

For a structure such as the Penrose lattice that is composed of two types of plaquettes with irrational area ratios, the plaquettes can never achieve their energy minima simultaneously as the magnetic field is varied, a phenomenon known as *geometrical frustration*.¹¹ The degree of frustration can be characterized by a parameter f , which is the ratio of the external flux in a plaquette to the quantum of flux. Only when f is an integer for all plaquettes can all junctions be simultaneously at minimum energy.

When the array is a periodic ladder and f is rational, the ground state is a superlattice of vortices. Vallat and Beck¹² showed that for the cosine interaction the energy $E(f)$ is a uniformly continuous function of f . The ground state energy $E(f)$ and the transition temperature $T_c(f)$ are both periodic functions of f , with distinct local minima where f is a simple rational, showing that commensuration is important for this case.¹³

Behrooz *et al.*⁷ considered the problem of flux quantization on a quasiperiodic network of thin aluminum wires. The network consisted of parallel evenly spaced wires in one direction, but with unevenly spaced parallel wires in the other. The latter spacing was generated by a substitution rule, so that it had inflation symmetry characterized by the irrational number $\sigma = 1 + \sqrt{2}$. The ratio of the areas of the two kinds of plaquettes in the quasicrystalline network was also σ . They found that $T_c(f)$ was no longer a periodic function of the frustration, but it did show a series of high peaks which in magnitude were nearly the same as that of the unfrustrated network.

We consider aperiodic ladders consisting of two types

of plaquettes with incommensurate areas, as in Fig. 1, and study the ground state energy spectrum as a function of frustration, $E(f)$. The critical temperature gives a measure of the ground state energy, and in this respect we, as with Behrooz *et al.*, find that the deep energy minima occur when it is simultaneously true that the magnetic flux through the large and small plaquettes is approximately an integer multiple of the flux quantum. We show that a model that treats the plaquettes independently describes these energy minima quite well. Considering the set of energy minima in $E(f)$, we find that a quasiperiodic function emerges, with this quasiperiodic property being dictated by the incommensurate areas and not the aperiodicity.

The structure of the paper is as follows. In Sec. II we introduce the Independent Plaquette Model. We begin our study of the aperiodic ladders in Sec. III. Conclusion comes as Sec. IV. An Appendix complements this study in that it provides a model with cosine interaction, having an analytic *fractal* solution for $E(f)$.

II. THE INDEPENDENT PLAQUETTE MODEL (IPM)

Consider first a Josephson junction ladder in a uniform perpendicular magnetic field. The hamiltonian for this system is

$$H = -E_J \sum_k [\cos(\theta_{1,k} - \theta_{1,k+1}) + \cos(\theta_{2,k} - \theta_{2,k+1}) + \cos(\theta_{1,k} - \theta_{2,k} - 2\pi f x_k)], \quad (2.1)$$

where $\theta_{1,k}$ and $\theta_{2,k}$ are the phases of the superconducting order parameter along the upper and lower sides of the ladder, respectively. We have chosen the gauge of the vector potential so that it has zero component along the horizontal junctions. Then the effects of the applied field are represented by $A_{ij} = \frac{2e}{\hbar c} \int_i^j A(\vec{r}) \cdot d\vec{l} = 2\pi f x_k$ where x_k is the x -coordinate of the k th vertical junction (a rung of the ladder). The frustration factor f is the flux through a plaquette of unit area, measured in units of the flux quantum.

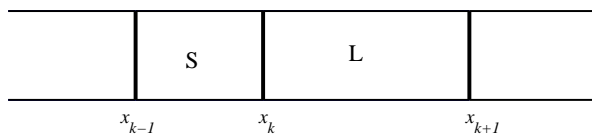


FIG. 1: Two kinds of plaquettes with different areas that are part of a Josephson junction ladder. The arrangement of such plaquettes in the ladder can follow an aperiodic sequence.

For a periodic ladder, the ground state energy is a periodic function of f . The energy takes on the unfrustrated

value (corresponding to the peaks in T_c) for values of f that can be understood by imposing the condition that no plaquette be frustrated.¹⁴ We will show that the “Independent Plaquette Model” is also useful for the aperiodic situation.

First, let us consider a single isolated plaquette containing four junctions; furthermore, let us choose the gauge so that A_{ij} has the same value for each successive junction as we go around the plaquette. Then we will have $A = \pi f S/2$, where S is the area of the plaquette, and the energy becomes

$$H = -\cos(\theta_1 - \theta_2 - A) - \cos(\theta_2 - \theta_3 - A) - \cos(\theta_3 - \theta_4 - A) - \cos(\theta_4 - \theta_1 - A), \quad (2.2)$$

where θ_i are the phases at successive sites of the ring. Analysis shows that the minima of H occur for θ_i such that $\theta_i - \theta_{i+1} = \pi n/2$ where n is an integer; the minimum energy per junction is given by

$$E = -\cos\left(\frac{\pi}{2}(fS - [fS])\right), \quad (2.3)$$

where $[x]$, throughout this paper, denotes the integer closest to x . It is readily seen that the minimum energy per junction occurs when fS is an integer, and that it is periodic in f with period $1/S$. Near a minimum, the cosine function is relatively insensitive to variations in the θ_i away from the optimum values. This suggests that even in an array, when one plaquette is close to its energy minimum it will not be greatly perturbed by its links to other sites, nor will its presence greatly perturb the other rings. Then we may attempt to approximate the ground state energy per junction for an interacting system by averaging the plaquette energies Eq. (2.3).

In the present case, the ladder has two types of plaquettes; L with area A_L , and S with area A_S . Let N_{Ladder} be the number of plaquettes in the ladder, N_L the number of plaquettes of type L , and N_S the number of plaquettes of type S . Then within the IPM the energy per junction of the ladder becomes

$$E_{IPM} = \frac{1}{N_{Ladder}} (N_S E_S + N_L E_L), \quad (2.4)$$

where $E_S(E_L)$ is the energy per junction for a plaquette of type $S(L)$. From 2.3 we can write:

$$E_S = -\cos\left(\frac{\pi}{2}(A_S f - [A_S f])\right), \quad (2.5)$$

$$E_L = -\cos\left(\frac{\pi}{2}(A_L f - [A_L f])\right). \quad (2.6)$$

It will prove convenient to choose A_S to have unit area (which sets the scale for f), and define $\alpha = A_L/A_S$ and $\nu = N_L/N_S$. Then the average spacing between vertical junctions (the rungs of the ladder) is

$$a = \frac{1 + \nu\alpha}{1 + \nu}, \quad (2.7)$$

and we can write Eqs.(2.5 – 2.7) as

$$E_{IPM} = \frac{1}{1+\nu}(E_S + \nu E_L), \quad (2.8)$$

$$E_S = -\cos\left(\frac{\pi}{2}(f - [f])\right), \quad (2.9)$$

$$E_L = -\cos\left(\frac{\pi}{2}(\alpha f - [\alpha f])\right). \quad (2.10)$$

We will not claim that the IPM is anything more than a crude approximation. Neighboring plaquettes are allowed to assign different currents to the rung they share; not only is this ignored, the rung energy is counted twice in the averaging! However, it is easy to use, and we will see that its predictions are not too different from the numerical simulations (to which it seems to serve as a lower bound). We will be particularly interested in the values for f for which the energy per junction is close to the absolute minimum $-E_J$, and for these cases the supercurrent on every junction is small, and the predictions of the IPM become accurate.

III. STUDY OF APERIODIC LADDERS

Here we compare a numerical study of the spectrum of the ground states of various frustrated Josephson junction ladders with the predictions of the IPM. Each ladder is a sequence of two kinds of plaquettes, L and S . This enables us to distinguish the importance of two properties of the ladder: the ratio of areas of the two kinds of plaquettes, and the order or particular arrangement of the plaquettes in the ladder.

The ground state energy $E(f)$ is found numerically using the Monte Carlo (MC) simulated annealing routine.¹⁵ A candidate ground state configuration is what is obtained at the lowest temperature attempted, which we have taken to be $T = 0.001$. (By this we mean $k_B T/E_J = 0.001$.)

We can detect any kind of order that might exist in ground state energy as a function of frustration, by calculating the “discrete power spectrum”¹⁶ for $E(f)$ known for N values of f in a range $-F \leq f \leq F$ ($E(f)$ is an even function of f , so the range can be doubled). The Fourier transform of $E(f)$ is

$$\begin{aligned} \hat{E}(\omega) &= \frac{1}{2F} \int_{-F}^F E(f) \exp(i2\pi f\omega) \\ &\approx \frac{1}{N} \sum_{n=0}^{N-1} E(nF/N) \exp(i2\pi nk/N) \end{aligned} \quad (3.1)$$

where $\omega = k/F$ with $k = 1 - N/2, \dots, N/2 - 1$. Then the discrete power spectrum is

$$S_\omega = (|\hat{E}_\omega|^2 + |\hat{E}_{-\omega}|^2), \quad (3.2)$$

To the extent that $E(f)$ can be represented as a sum of periodic components, $S(\omega)$ will have peaks at the corresponding frequencies.

For better comparison, we define an incomplete sum over frequencies as

$$IS_{\omega=j/F} = \sum_{k=1}^j S_k. \quad (3.3)$$

When at a frequency j the power spectrum has a peak, the incomplete sum of the discrete power spectrum has a jump. Therefore, jumps in IS_ω indicate peaks in S_ω , with the size of the jump indicating the summed weight of the peak. In the results to be presented we used an increment of 1/13 in frustration and 256 data points, except for the case of σ Fibonacci where we had an increment of 1/55 and 5500 points.

The power spectrum was calculated in MATLAB by the FFT method.¹⁷

A. τ Fibonacci Ladder

We start with a ladder made of two types of plaquettes, with area ratio τ and arranged according to the Fibonacci sequence; we call this the τ Fibonacci ladder. The plaquette areas are $A_L = \tau = (1 + \sqrt{5})/2$ and $A_S = 1$. Denoting the structure in its n th step of construction by U_n , the structure is constructed recursively by the rule $U_{n+2} = U_{n+1} + U_n$, where summation means adjacent placement: to get the structure in step $(n+2)$, put the structure in step $(n+1)$ first, and that of step n , to its right. This generates the sequence

$$S, L, LS, LSL, LSLLS, LSLLSLSL, \dots \quad (3.4)$$

In the limit of an infinite structure this defines a quasicrystalline ladder with $\nu = \tau$.

The quasiperiodic grid defining the sequence of long and short spacings for our τ Fibonacci ladder is given by¹⁸

$$x_n = n + \delta + \tau^{-1}[\tau^{-1}n + \beta]. \quad (3.5)$$

where δ and β are arbitrary constants, chosen to be $\delta = 0$, $\beta = -1/2$.

Within the IPM each plaquette minimizes its energy by itself; in this way the expression for the energy becomes

$$E_{IPM} = -\frac{1}{1+\tau} \cos\left(\frac{\pi}{2}(f - [f])\right) - \frac{\tau}{1+\tau} \cos\left(\frac{\pi}{2}(\tau f - [\tau f])\right). \quad (3.6)$$

Eq. (3.6) is composed of two terms; the first has period $\Delta f = 1$, while, the second has period $\Delta f = 1/\tau$. Hence this function attains its minima for those f which are close to integers and which bring τf close to an integer. These include the Fibonacci numbers 2, 3, 5, 8, 13, 21, but there are other values of f ($f = 6.11, 6.88, 11.08, \dots$ that also meet this criterion. Even though the energy as a function of frustration is not periodic, it shows order in its structure. For example, the energy spectrum between the special values of f that minimize frustration is nearly symmetric about the midpoint; e.g. $E(5+x) \simeq E(8-x)$.

The numerical calculation of the ground state energy is given in Fig. 2 along with the predictions of Eq. (3.6). It is not surprising that $E_{IPM} < E_{MC}$, because the IPM neglects the interaction between the plaquettes. However, most features of the numerical curve are reproduced by the IPM. We can quantify this comparison by calculating the incomplete integral of power spectra, shown in Fig. 3.

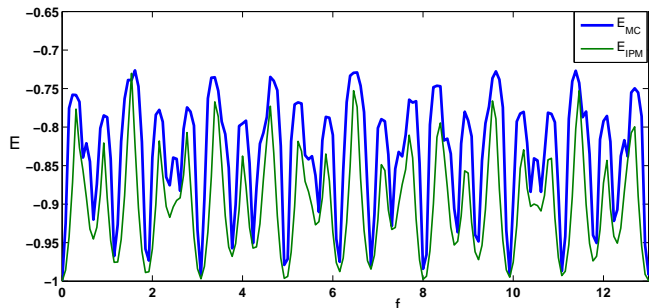


FIG. 2: Energy for the τ Fibonacci ladder. The area ratio is $\tau = (1 + \sqrt{5})/2$ and the order of the plaquettes is determined by the Fibonacci sequence. The upper curve is the ground state energy as determined by simulated annealing; the lower curve is the result of the Independent Plaquette Model (IPM) approximation.

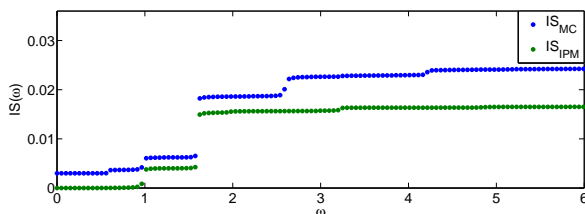


FIG. 3: Incomplete sum of the Fourier spectrum of $E(f)$ for the τ Fibonacci ladder using the numerical minimization (top) and the IPM (bottom). The top figure shows jumps at $\omega = \tau - 1, 1, \tau, \tau + 1$. This shows that the energy is quasiperiodic as a function of f , with periodicities $\Delta f = \tau^{-2}, \tau^{-1}, 1$, and τ , and weaker periodicities at various integer combinations of unity and τ . Figures are shifted relative to each other, for clarity.

Both $E(f)$ contain significant periodicity corresponding to the frequencies $\omega = 1$ and $\omega = \tau$. While the IPM energy expression is a sum of two periodic functions with incommensurate periods, the numerical result indicates that this function is quasiperiodic too, as it also includes the sum and difference of the frequencies in the power spectrum: $\tau + 1$ and $\tau - 1$. This is also what is found for the tight binding hamiltonian model on a Penrose lattice.¹⁹

B. σ Fibonacci ladder

We have seen that the quasiperiodic nature of the sequence and the special ratio of the areas both play roles in the power spectrum. To distinguish the role of the area ratio from the effects of the sequence we will keep the Fibonacci order for the arrangement of the S and L plaquettes, but choose the areas to be in the silver ratio: $A_L = \sigma = 1 + \sqrt{2}$ and $A_S = 1$. The general formula for generating this ladder is now¹⁸

$$x_n = n + \delta + \left[\frac{n}{\tau} + \beta\right]\sqrt{2}, \quad (3.7)$$

with δ and β being arbitrary, chosen here to be $\delta = 0$, $\beta = -1/2$.

For this ladder the energy within the IPM is expressed as,

$$E_{IPM} = -\frac{1}{1+\tau} \cos\left(\frac{\pi}{2}(f - [f])\right) - \frac{\tau}{1+\tau} \cos\left(\frac{\pi}{2}(\sigma f - [\sigma f])\right). \quad (3.8)$$

Figure 4 shows the result of a simulated annealing Monte Carlo study of the ground state energy for a ladder with 144 plaquettes, along with the predictions of the IPM, Eq. (3.5). The properties mentioned for the τ Fibonacci ladder hold here too: there are minima near $f = 2, 3, 5, 7, 10$, and 12 because for these values σf is also close to an integer. The comparison of the Fourier

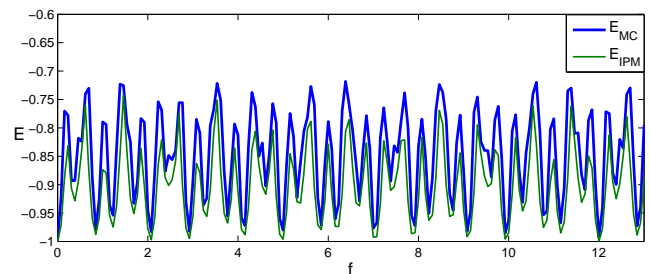


FIG. 4: Energy for the σ Fibonacci ladder. The area ratio is $\sigma = 1 + \sqrt{2}$ and the order of the plaquettes is determined by the Fibonacci sequence. The upper curve is the ground state energy as determined by simulated annealing; the lower curve is the result of the Independent Plaquette Model approximation.

spectra for the two energy plots, Fig. 5, indicates that the dependence of the energy on f is dictated by σ and not by the specific way the plaquettes are arranged. The ratio of the areas causes the frustration, and the energy minima occur for the values of f that give nearly integer flux through each plaquette. The quasiperiodic nature of $E(f)$ indicates that there is a fine structure to it that corresponds to a ‘many tile effect,’ pointing to the presence of vortex lattices commensurate with the underlying structure.^{4,20} The IPM cannot predict this effect, and in Fig. (5) we have peaks that are not reproduced by the independent plaquettes approximation, just as in the case of Fig. (3).

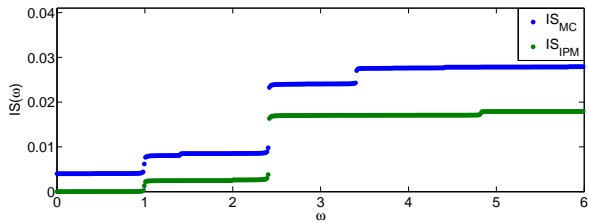


FIG. 5: Similar to Fig. 3 but when $E(f)$ is for the σ Fibonacci ladder. The jumps at $\omega = \sigma - 1, 1, \sigma, \sigma + 1$ show that the energy is quasiperiodic as a function of f , with periodicities $\Delta f = (\sigma+1)^{-1}, \sigma^{-1}, 1$, and $(\sigma-1)^{-1}$, and weaker periodicities at various integer combinations of unity and σ . Figures are shifted relative to each other for clarity.

C. Other τ Ladders

To further study the importance of plaquette order, we have considered three ladders with $\nu = 1$ and $\alpha = \tau$, having different arrangements of the S and L plaquettes: random order, the Thue–Morse sequence,²¹ and a periodic lattice.

For the random ladder, the results for a simulation using 144 plaquettes is shown in Fig. 6. According to our simulated annealing study, there is less fine structure in the random ladder than predicted by the IPM. It remains true that the IPM consistently gives a slightly lower energy than the simulated annealing, and that it locates the energy minima. The incomplete integral of the power spectrum of the τ Random $E(f)$ is shown in Fig. 7; the other two τ Ladders mentioned here give similar results.

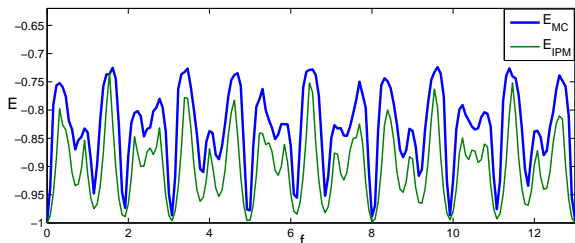


FIG. 6: Energy for the τ Random ladder. The area ratio is $\tau = (1 + \sqrt{5})/2$ and the order of the plaquettes is determined by the random sequence. The upper curve is the ground state energy as determined by simulated annealing; the lower curve is the result of the Independent Plaquette Model (IPM) approximation.

We have also studied the τ Periodic lattice (a periodic sequence of SL , with areas having ratio τ). as well as one having the Thue–Morse order (built recursively by appending the complement of a sequence to itself: $SL, SLLS, SLLSLSL, \dots$). Our results are summarized in Table I for the numerical results and Table II for the IPM results. We see that all lattices have peaks

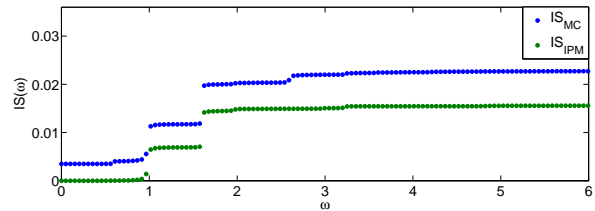


FIG. 7: Periodicity of $E(f)$ for the τ Random ladder, as represented by the incomplete integral of the power spectrum (similar to Fig. 3). It shows jumps at $\omega = \tau - 1, 1, \tau, \tau + 1$. This shows that the energy is quasiperiodic as a function of f with periodicities $\Delta f = \tau^{-2}, \tau^{-1}, 1$, and τ , and weaker periodicities at various integer combinations of unity and τ . The characteristics in this figure are nearly identical with those of the other two τ Ladders. Figures are shifted relative to each other, for clarity.

at $\omega = 1, \alpha$ and $\alpha \pm 1$, and this shows that $E(f)$ is a quasiperiodic function with main peaks at $\omega = 1$ and α . From these results we separate out the role of the areas of plaquettes from that of the order in lattice. τ Fibonacci and σ Fibonacci lattices have the same order but with different areas of plaquettes. The results for these two lattices show that the position of the main peaks is determined by the areas of plaquettes.

We can further justify the results by a quantitative argument that starts with the IPM model. From the IPM model we know that the main peaks in $S(\omega)$ are proportional to the square of the density of S and L . These are just the coefficients of E_S and E_L , in the expression for energy (Eqs. 2.8–2.10). Then the peak heights depend only on ν ; this is why the last three rows of Table II (for different $\nu = 1$ models) have identical entries for the corresponding peaks. In the same way, we can explain the added peaks in the MC data of Table I in terms of the correlations between plaquette types. We define D_{LS} to be the probability that the two types of plaquettes appearing adjacent to each other: the ratio of all possible LS and SL pairs to the total possible number of pairs in the array. This is correlated with the height of the peaks at $\omega = \alpha + 1$, as shown in Table III. For the τ ladders, the peak height is proportional to D_{LS} to good approximation. There is a similar explanation²² for the amplitudes of the peaks at $\omega = \tau - 1$ that uses the LS combination as its basic unit, so that two-plaquette interactions account for this case, too.

In summary, our study of the one dimensional lattices shows that $E(f)$ is a quasiperiodic function with the main frequencies at the areas of the plaquettes. This property is an extension of that of the periodic behavior for the square lattice.²³ We can also observe an approximate mirror symmetry in the dependence of E on f ; by that we mean, there is a set of values f_n for which the energy is very close to its unfrustrated value, and between these values $E(f)$ has a mirror symmetry about $f = (f_n + f_{n+1})/2$. This can again be viewed as an ex-

τ Fibonacci	$\tau-1$ (0.653)	1 (2.360)	τ (12.14)	$\tau+1$ (3.518)
σ Fibonacci	1 (3.457)	$\sigma-1$ (0.397)	σ (14.0)	$\sigma+1$ (3.249)
τ periodic	$\tau-1$ (0.565)	1 (7.132)	τ (8.111)	$\tau+1$ (3.899)
τ Thue-Morse	$\tau-1$ (0.422)	1 (10.16)	τ (9.387)	$\tau+1$ (2.334)
τ Random	$\tau-1$ (0.5285)	1 (7.138)	τ (8.164)	$\tau+1$ (1.455)

TABLE I: Peak locations and heights for different lattices, according to the simulation. For each lattice four main peaks given; number in parentheses gives height of peak (we multiply it by 1000 for better representation).

τ Fibonacci	1 (4.208)	τ (11.008)
σ Fibonacci	1 (4.208)	σ (11.008)
τ periodic	1 (7.2)	τ (7.2)
τ Thue-Morse	1 (7.2)	τ (7.2)
τ Random	1 (7.2)	τ (7.2)

TABLE II: Peak locations ω and heights (in parentheses) for different lattices, according to the IPM. For each lattice two main peaks given; number in parentheses gives height of peak (we multiply it by 1000 for better representation).

tension of the mirror symmetry for the square lattice.

IV. CONCLUSION

The independent plaquette model treats the plaquettes as if they were independent of each other, and at the deep energy minima, this nearly coincides with the energy minimum when such an approximation is lifted.

By using the numerical minimization of Hamiltonian 2.1 we find some interesting results about the structures of ground state energy $E(f)$. We see that $E(f)$ has two main frequencies and their ratio equals the ratio of areas of the two plaquettes. There are other frequencies in the spectrum of $E(f)$ equal to sum and difference of the two main frequencies, indicating that $E(f)$ is a quasiperiodic function and not just a sum of two periodic functions with incommensurate periods. The order of the lattice affects the amplitudes of different frequencies in the spectrum of $E(f)$. Study of the energy power spectrum gives a role to the lattice ordering because this affects the correlations

τ Fibonacci	$2/\tau^2$	6.028
σ Fibonacci	$2/\tau^2$	5.567
τ periodic	1	5.899
τ Thue-Morse	$2/3$	5.252
τ Random	$1/2$	5.820

TABLE III: The ratio of all possible LS and SL pairs to the total possible number of pairs in the array is defined as D_{LS} , and given in first column. The second column gives the ratio of $S(\alpha+1)$ to D_{LS}^2 (we multiply it by 1000 for better representation).

between S and L , which goes beyond the IPM. However, this is only a short range effect; we have no evidence that the long range order in the array plays any role.

If we look at the behavior of $T_c(f)$, which roughly goes hand in hand with the ground state energy, the linearized mean-field theory provides an analytical approach to the problem.²⁴ The results of this model show that $T_c(f)$ is a quasiperiodic function.²⁵ In their respective Fourier spectra, we observe peaks on the same special combinations of the main frequencies, and this is an indication of the particular order present in the lattice.

The independent plaquette model provides an excellent approximation for $E(f)$, following nearly all its features, while apparently giving a lower bound for it.

Acknowledgement

Y.A. and M.R.K. acknowledge the support of a grant from the Institute for Advanced Studies in Basic Sciences.

APPENDIX: IPM and the J^2 model

In a study with similar motivation, Grest, Chaikin and Levine²⁶ (GCL) numerically studied the ground states of a one dimensional quasiperiodic array with inflation symmetry. Although their model was inspired by the Josephson network, it differed from it in two ways:

*They simplified the form of the interaction, in effect replacing $\cos(x)$ by $1 - \frac{1}{2}(x - 2\pi n)^2$ (where n is the integer that gives the minimum value for this expression²⁷). In practice the arguments of the cosine function are small (mod 2π), so that this is a good approximation; it somewhat changes the energy cost of introducing a vortex, but this is unimportant since the number of vortices is set by the applied field. They refer to this as the ‘‘current squared’’ (J^2) model.

*They assumed that no current is carried along the periodic wires.²⁸ This forces the phases along these wires to be all the same (in a certain gauge), and implies that all plaquettes along a column either all contain a vortex or all do not. This reduces the mathematics problem to one dimension, so that Griffiths and Floría²⁹ (GF) were able to solve the model exactly. In their numerical study, GCL found that there are deep minima in $E(f)$ which they interpreted as due to a kind of commensuration between the current pattern and the underlying lattice. Similar results were found in experimental studies by Chaikin et al.²⁰ For the J^2 model, GF showed that $E(f)$ takes on the value $1 - \pi^2/3$ (the averaged value of the approximated cosine function) for almost all f , but that there is a countable set of irrational values of f at which $E(f)$ takes on a lower value.

We have some misgivings about the choice of model. The way that GCL reduce it to one dimension does some violence to the physical situation. A column of vortices is unstable, because the vortices repel each other. We

would expect that the ground state configurations would have the vortices more uniformly spaced in two dimensions. Having no current on the periodic wires also means that the current is the same on all of the nonperiodic wires and does not vary along it. We will show that with this very strong constraint, it is not necessary to make the J^2 approximation: the model can be exactly solved for the cosine interaction (with very little difference in the results).

The GCL model is defined by the energy function

$$H = -E_J \sum_{i,j} [\cos(\theta_{i,j} - \theta_{i+1,j}) + \cos(\theta_{i,j} - \theta_{i,j+1} - 2\pi f x_i)]. \quad (\text{A-1})$$

As an approximation, GCL assumed $\theta_{i,j}$ to be independent of i , which implies that there is no current along the “horizontal” links corresponding to the index i . This makes the first term a constant which will not be included in what follows. Minimizing the energy with respect to θ_j gives

$$\sin(\theta_j - \theta_{j+1} - 2\pi f x_i) = \sin(\theta_{j-1} - \theta_j - 2\pi f x_i), \quad (\text{A-2})$$

which implies $\theta_j - \theta_{j+1} = \theta_{j-1} - \theta_j \pmod{2\pi}$. Then there is just one undetermined variable: the difference in phase b between adjacent columns. Specification of b determines all of the currents and link energies in the form

$$E = - \lim_{N \rightarrow \infty} \frac{1}{N} E_J \sum_{j=1}^N \cos(b - 2\pi f x_j). \quad (\text{A-3})$$

This is not the same as the model that we have been discussing, but the results can be compared to those of the IPM. Applying the IPM to the two-dimensional array again leads to Eqs. (2.8 – 2.10) since it decouples neighboring plaquettes.

Eq. (A-3) can be evaluated exactly following the methods of GF. They define $r(y)$ to be the distribution of the

values $y_j = f x_j \pmod{1}$, so that the energy can be calculated from

$$E = -E_J \int_0^1 \cos(2\pi y) r(y - b) dy. \quad (\text{A-4})$$

They consider sequences $\{x_j\}$ that can be written in the form $x_i = a[i + g(i\omega)]$ where $g(x)$ is the periodic extension (with period 1) of the function $g(x) = \gamma x$. These include the periodic, τ , and σ ladders — for example, the τ ladder corresponds to $a = 3 - \tau$, $\gamma = 1/\sqrt{5}$, and $\omega = \tau - 1$. They show that for almost all values of f , $r(y)$ is the uniform distribution $r(y) = 1$ (so that $E = 0$), but that $r(y)$ has nontrivial form for $af = (l + m\omega)/n$, where l , m , and n are integers and a sets the scale. The effects for $n > 1$ are relatively small and will not be considered further. Then

$$r(y) = (K + 1)/\kappa \quad \text{for } -s/2 < y < s/2, \quad (\text{A-5})$$

$$= K/\kappa \quad \text{otherwise.} \quad (\text{A-6})$$

Here, we have $s = \kappa - K$, with $\kappa = |(1 + \gamma\omega)m + \gamma l|$, and K the largest integer less than κ . The corresponding energy is³⁰

$$E = -E_J |\sin(\pi\kappa)/\pi\kappa|. \quad (\text{A-7})$$

Because GF follow GCL making the approximation $\cos(x) = 1 - x^2/2$, they obtain a slightly different result.

It is readily seen that the most negative values for Eq.(A-7) occur when κ is small, i.e. when $m/l \approx |1 + \gamma\omega|/|\gamma|$. The dependence of the energy on f described by Eq.(A-7) is a discontinuous fractal function — a forest of vertical lines, rather than the smooth curves we find numerically for the Josephson ladder. We believe this to be a real difference between the two models. In any case, the two results agree on the positions of the deepest minima.

¹ M. Kohmoto, B. Sutherland, and C. Tang, Phys. Rev. B **35**, 1020 (1987).

² K. Niizeki and T. Akamatsu, J. Phys. Condens. Matter **2**, 2759 (1990).

³ B. D. Biggs, Y. Li, and S. J. Poon, Phys. Rev. B **43** 8747 (1991).

⁴ J. Q. You, L. Zhang, and Q. B. Yang, Phys. Rev. B **55**, 1314 (1997).

⁵ H. Tsunetsugu, T. Fujiwara, K. Ueda, and T. Tokihiro, Phys. Rev. B **43**, 8879 (1991); K. Niizeki and T. Akamatsu, J. Phys. Condens. Matter **2**, 7043 (1990); B. Sutherland, Phys. Rev. B **34**, 3904 (1986).

⁶ W. A. Little and R. D. Parks, Phys. Rev. Lett. **9**, 9 (1962).

⁷ B. Pannetier, J. Chaussy, R. Rammal, and J. C. Villégier, Phys. Rev. Lett. **53**, 1845 (1984); A. Behrooz, M. J. Burns, H. Deckman, D. Levine, B. Whitehead, and P. M. Chaikin, Phys. Rev. Lett. **57**, 368 (1986).

⁸ F. Nori, Q. Niu, E. Fradkin, and S.-J. Chang, Phys. Rev. B **36**, 8338 (1987); V. Misko, S. Savel’ev, and F. Nori, Phys. Rev. Lett. **95**, 177007 (2005).

⁹ S. Teitel and C. Jayaprakash, Phys. Rev. Lett. **51**, 1999 (1983); M. R. Kolahchi and J. P. Straley, Phys. Rev. B, **43**, 7651 (1991).

¹⁰ G. Toulouse, Commun. Phys. (G. B.) **2**, 115 (1977).

¹¹ J-F. Sadoc and R. Mosseri, *Geometrical Frustration*, (Cambridge University Press, 2006).

¹² A. Vallat and H. Beck, Phys. Rev. Lett., **68**, 3096 (1992).

¹³ J. P. Straley and G. M. Barnett, Phys. Rev. **B 48**, 3309 (1993).

¹⁴ M. R. Kolahchi and J. P. Straley Phys. Rev. **B 66**, 144502 (2002)

¹⁵ N. Metropolis, A. Rosenbluth, M. Rosenbluth, A. Teller, and E. Teller, J. Chem. Phys., **21**, 1087 (1953); S. Kirkpatrick, C. D. Gelatti, and M. P. Vecchi, Science, **220**, 671

- (1983).
- ¹⁶ Chapters 12 and 13 in *Numerical Recipes: The Art of Scientific Computing* by William H. Press, Saul A. Teukolsky, William T. Vetterling and Brian P. Flannery, Cambridge UP 3rd Ed. 2007.
- ¹⁷ E. W. Weisstein, *Fast Fourier Transform*, from MathWorld—A Wolfram Web Resource. For Fourier transform and complexity of quasiperiodic sequences see, F. Axel and D. Gratias, *Beyond Quasicrystals*, (Springer, 1995), pp. 331-351.
- ¹⁸ J. E. S. Socolar and P. J. Steinhardt, *Phys. Rev. B*, **34**, 617 (1986).
- ¹⁹ H. Schwabe, G. Kasner, and H. Böttger, *Phys. Rev. B*, **56**, 8026 (1997).
- ²⁰ P. M. Chaikin, A. Behrooz, M. A. Itzler, C. Wilks, B. Whitehead, G. Grest, D. Levine, *Physica B*, **152**, 113 (1988).
- ²¹ R. Merlin, K. Bajema, J. Nagle, K. Ploog, J. de Physique **48**, C5-503 (1987).
- ²² Y. Azizi, Unpublished.
- ²³ C. J. Lobb, *Physica B*, **126**, 319 (1984).
- ²⁴ W. Y. Shih and D. Stroud, *Phys. Rev. B*, **28**, 6575 (1983).
- ²⁵ Q. Niu and F. Nori, *Phys. Rev. B*, **39**, 2134 (1989).
- ²⁶ G. S. Grest, P. M. Chaikin, D. Levine, *Phys. Rev. Lett.*, **60**, 1162 (1988).
- ²⁷ References 19, 25, and 28 chose to define their models in terms of functions of unit period, whereas we use functions with period 2π . We have translated their results into our notation.
- ²⁸ This approximation is not a necessary part of the J^2 model.
- ²⁹ R. B. Griffiths and L. M. Floría, *Phys. Rev. B*, **45**, 9887 (1992).
- ³⁰ To be compared with a similar result for the diffraction pattern of a 1D quasicrystal, in D. Levine and P. J. Steinhardt, *Phys. Rev. B*, **34**, 596 (1986).